Covid-19 and Pneumonia Infection Detection from Chest X-Ray Images using U-Net, EfficientNetB1, XGBoost and Recursive Feature Elimination

Munindra Lunagaria, Vijay Katkar, Krunal Vaghela
Department of Computer Engineering
Marwadi University
Rajkot, India

***Abstract*—The pandemic caused by the COVID-19 virus is the most serious current threat to the public's health. For the purpose of identifying patients with Covid-19, Chest X-Rays have proven to be an indispensable imaging modality for the hospital. Nevertheless, radiologists are needed to commit a significant amount of time to their interpretation. It is possible to diagnose and triage cases of Covid-19 effectively and rapidly with the assistance of precise computer systems that are powered by Machine Learning techniques. Machine Learning techniques such as Deep Feature Extraction can help detect the disease with improved precision and speed when used in conjunction with X-Ray images of the lung. This helps to alleviate the problem of lack of testing kits. Using the U-Net for Semantic image segmentation for lung segmentation and deep feature extraction-based strategy that was suggested in this research, it is possible to differentiate between patients who have contracted the Covid-19 virus, pneumonia and healthy people. XGBoost and recursive feature extraction based proposed methodology is evaluated using 20 different Pre-Trained deep learning based models including EfficientNet variations and it is observed that the maximum detection accuracy, precision, recall specificity, and F1-score are achieved when EfficientNetB1 is used to extract deep features. The respective values for these metrics are 97.6%, 0.964, 0.964, and 0.982. These findings lend credence to the efficiency of the proposed methodology.**

***Keywords*—Covid-19; u-net; efficientnet; semantic image segmentation; XGboost; recursive feature extraction**

I. Introduction

The recently found Coronavirus pneumonia, which has been given the name Covid-19 ever since it was found, is both extremely contagious and highly pathogenic [1]. The symptoms may advance to a more unadorned form of pneumonia, which can lead to serious health problems and the failure of multiple organs. There is also the risk that pneumonia will prove fatal to the patient. Covid-19 has spread to 223 nations and is blamed for over 6.4 million deaths around the earth; additionally, quantity of deaths caused by virus is steadily rising [2] (see Fig. 1). In any region of the world, medical professionals, governments, organizations, and countries face a noteworthy impediment in the form of need to diagnose Covid-19 patients as early as possible.

Even though immunological tests are offered in a number of countries, the RT-PCR i.e., Real-Time Reverse Transcription-Polymerase Chain Reaction is the process that is employed majority of the time to identify Covid-19. Early treatment can be ensured by recognizing the detrimental effects of Covid-19 by assessing photographs of patients' lungs rather than relying on RT-PCR, which has limited sensitivity (60–70%) and is also a technology that requires a significant amount of time.

Care for patients with Covid-19 necessitates careful tracking of their condition's evolution over time. When used in conjunction with other diagnostic tests, medical imagery practices like Computed Tomography (CT) and X-Rays of Chest can help to confirm a diagnosis of Covid-19 pneumonia and keep tabs on how the disease is progressing. These photos demonstrate the rapid progression of ground-glass opacities with irregular patterns after the onset of Covid-19 symptoms [3].

The term “Artificial Intelligence” (AI) refers to an assorted methodologies intended at imitating human cognition and deeds. Algorithms that consent high end processers to comprehend intricate patterns and associations from empirical information are the focus of the discipline of Machine Learning (ML), a subfield of AI. While traditional ML approaches are limited in their ability to deal with complicated problems like medical image categorization, Deep Learning (DL) takes cues from biological neural networks to attain greater power and flexibility [4].

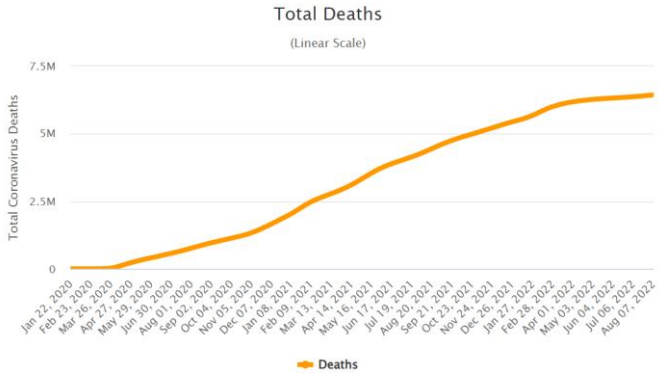

Fig. 1. Number of Worldwide Deaths Due to Covid-19.

Having access to a big dataset that contains images that have been labeled is essential to the success of a detection or classification system that is based on DL. Deep feature extraction (DFE) and transfer learning (TL) are two of the most successful alternatives to using a small sample size of images when there is not a big sample size of images available. TL refers to the process of making use of previously taught models to tackle unanticipated obstacles. TL is not an individual category of ML algorithms; rather, it is a process that can be utilized in the development of a new ML model. Model will be able to put the knowledge and abilities that it has gained in previous training to use in brand new situations [5]. In a manner analogous to the activity that came before it, this one will need organizing data according to the type of file. Another application of TL is the extraction of deep feature information. It is possible to extract feature vectors by making use of pre-trained CNN models rather than manually adjusting the activation layers of the CNN. The deeper layers, which are triggered by the activations of the lower-level layers, include the higher-level features that are essential to the classification of images [6].

Using U-Net, EfficientNetB1, XGBoost and Recursive Feature Elimination (RFE), this paper provides a DFE-based technique for discriminating healthy individuals and those infected with pneumonia from those infected with Covid-19. The remaining paper is structured as follows. The relevant work is briefly described in Section II, and use of U-Net model is explained in Section III. Brief introduction of Pre-Trained models employed in the study is provided in Section IV. The proposed approach is explained in Section V whereas dataset utilized for the experiment along with experimental findings is described in Section VI. Section VII briefly describes the significant contributions of the research work whereas section VIII concludes the research work.

II. Literature Survey

CNNs are constructed by first adding a sequence of layers that are known as convolutional, then adding layers that are known as normalization, and finally adding layers that are known as pooling. Feature extraction is the responsibility of the convolution layers, whereas feature normalization and feature down sampling are the purview of the normalization and pooling layers, respectively. In a manner analogous to that of more traditional approaches to machine learning, training of the CNN is carried out by use of an optimization strategy like Stochastic Gradient Descent [7].

A DL-based framework with fuzzy enhancements was presented by Cosimo Ieracitano et al. [8] under the name CovNNet for the purpose of classifying Chest X-Rays of Covid-19 patients and recognizing those of other patients with pneumonia. The CovNNet model was given X-Rays of the chest as well as fuzzy images that were created using a fuzzy logic based edge detection method. Experiments have shown that using fuzzy features in conjunction with chest X-Rays can result in enhanced classification performance.

Emtiaz Hussain et al. [1] have introduced a 22-layer deep CNN model named CoroDet with the purpose of being utilized in the process of recognizing Covid-19 cases in chest CT and X-Ray images. Their methodology is validated for its usefulness utilizing a five-fold cross-testing procedure. Patient detection method using X-Ray pictures that is based on a faster RCNN-based object detection methodology was proposed.by Fátima A. Saiz and Iñigo Barandiaran [9].

To develop a concatenated neural network, Mohammad Rahimzadeh and bolfazl Attar [10] merged features extracted with ResNet50V2 and Xception, then transmitted the aggregated data to a convolutional layer. The convolutional layer is responsible for the extraction of features, and it uses 1024 filters with a Kernel size of 1x1. This layer is introduced in order to provide assistance to the network in better learning characteristics from the combined data. They demonstrated the viability of their approach by utilizing a procedure known as three-way cross-testing.

Arman Haghanifar et al. [11] compiled a significant number of different chest X-Ray images from a variety of sources into a single extensive database that is open to the public. The TL paradigm is used in conjunction with the CheXNet model to generate a model that is referred to as COVID-CXNet. This model is effective at detecting pneumonia caused by the coronavirus and pinpointing its exact location.

Mohammad Shorfuzzaman et al. [12] describes an ensembled-based DFE approach as a means of determining the existence of Covid-19 in X-Ray of chest images. This technique takes the weights that were determined by a large number of models that have been pre-trained and turns them into a single band that represents X-ray characteristics. After that, these traits will be utilized in the process of making a diagnosis of the ailment.

M. D. Kamrul Hasan et al. [13] suggest a two-stage, DFE-based process that makes use of VGG16 Net and patient lung X-Ray photos in order to sense COVID-19-induced pneumonia. When evaluating their methodology, the scores for precision, specificity, and sensitivity are taken into consideration.

Junfeng Li et al. [14] developed COVID-GATNet with the intention of identifying Covid-19 patients with the assistance of Graph Attention Network. The results of the X-Ray input can be interpreted as normal, as having Covid-19 +, or as having pneumonia. They used the information from three different open-source datasets to produce a more extensive training data pool for their studies.

Debabrata Dansana et al. [15] proposed a three-stage approach by utilizing CNN, Pre-Trained CNN models, and Decision Tree. The first step in the process is to use CNN to clean up the input images by removing any noise that isn't wanted and building composite feature maps. The performance of the pre-trained CNN models that are used to extract image features is improved with the help of these Composite feature maps, which are used in the second step. Second stage extracts image features to use for training a Decision Tree, which will be used for categorizing the disease.

According to research that was carried out by Karim Hammoudi et al. [16] who optimized four different Pre-Trained CNN models (specifically ResNet50, InceptionResnetV4, Densenet, and VGG-19), InceptionResnetV2 had the lowest

false negative rate. Abdullahi Umar Ibrahim et al. [17] showed that optimizing the Alexnet Pre-Trained model for patient detection in X-Ray pictures led to the discovery that the model is capable of providing good detection precision. Asif Iqbal Khan et al. [18] developed a TL-based model utilising Xception Net and gave it the name CoroNet. Xception Net's base layers are connected to the dropout layer, which is in turn coupled to fully-connected layers for classification task. A DFE-based approach employing the VGG-19 Pre-Trained Model was presented by Harsh Panwar et al [19]. The original VGG-19 model's foundational layers were expanded with fully connected layers, and they were then fine-tuned for patient detection.

Eduardo Luz et al. [20] presented DFE based method of hierarchical classification with the help of EfficientNet models. Target categories are positioned at leaves of the tree, whereas classifiers are located in the in-between nodes of the tree. At the root node, one classifier was used to segregate between the Normal and Pneumonia patients, while at a higher level, another classifier was used to segregate between the Pneumonia patients themselves.

Two-stage DFE based model for Covid patient detection using U-Net and Pre-Trained models was presented by Sivaramakrishnan Rajaraman and Sameer Antani [21]. After using U-Net to identify and extract the lung region in a chest X-ray, the resulting cropped pictures are fed back into the Pre-Trained model to be fine-tuned for improved detection accuracy.

Numerous studies have adopted a mixed-method approach, employing both traditional Data Mining based models like Support Vector Machine (SVM) and Pre-Trained DFE-based models for feature extraction in order to identify Covid-19 infected patients. Sara Hosseinzadeh Kassani et al. [22] presents a DFE based hybrid for computer-assisted decision of Covid-19 pneumonia. Several ML algorithms were trained on deep features extracted by well-known Pre-trained CNNs architectures. Their results suggests that hybrid approach is effective for computer-assisted detection.

A. Research Gap

Researchers put forth a lot of time and effort studying how best to detect Covid-19 using deep learning methods. A few research gaps remain, though, as can be seen below.

- Deep learning-based models trained for differentiating pneumonia from Covid-pneumonia fall into the category of Black box models.
- Existing methodologies use complete X-Ray images for detection of disease. X-Ray image contains many body parts other than lung which makes model less reliable.
- Researchers have not considered False Discovery Rate, Negative Predictive Value, False Negative Rate and False Positive Rate while evaluating their proposed model.

This paper resolves these research gaps with the help of U-Net model and Local Interpretable Model-agnostic Explanations methodology.

III. U-Net

U-Net was originally developed and used in 2015 to process biomedical images; it is an evolution of the conventional convolutional neural network [23]. The network's architecture was improved and expanded from the fully convolutional network to allow it to function with less training images and produce more accurate segmentations. The key concept is to add on more layers to a standard contracting network, with up sampling operators replacing pooling functions. This is because these layers improve the output's resolution. Later convolutional layers can use this data to fine-tune their outputs. U(up sampling) Net's section, which has been modified to include several feature channels, is what allows the network to convey contextual information to finer-grained nodes. This results in a u-shaped layout, with the expanding section mirroring the contracting one.

In this paper, the U-Net architecture is utilized for lung segmentation in patient Chest X-Rays. U-Net model's output for lung segmentation is displayed in Fig. 2. Raw X-Ray image is displayed in Fig. 2(a), while the result of the segmentation process is displayed in Fig. 2(b).

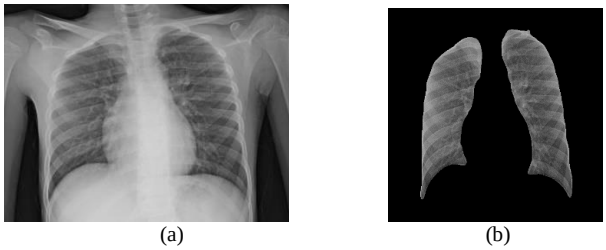

(a) (b)

Fig. 2. (a) Original X-Ray Image, (b) Output of U-Net.

From Fig. 2, it is clear that the segmentation process eliminates a great deal of inessential data from the X-Ray image.

IV. Deep Learning-based Pre-Trained Models

DFE has been widely implemented in the arena of medical imaging in current years. When compared to a CNN that has just been taught, a CNN that has undergone prior training and has undergone appropriate fine-tuning may perform better or on par with the latter. DFE has been vigorously explored for the goal of identifying Covid-19 in chest X-Rays, but there is a dearth of sufficient training data. This section briefly describes the most widely used Pre-Trained models for DFE by researchers.

A. MobileNet

It is extremely tiny CNN, making it ideal for integration into small form factors and embedded systems. By using depth-wise distinguishable convolution, a more lightweight architecture is built. Additionally, trade-off hyperparameters are introduced in order to find a fair equilibrium between accuracy and latency [24].

B. DenseNet

The term "Densely connected convolutional network" (also known as "DenseNet") refers to the architecture of a network in which every layer is capable of communicating directly with every other layer. Instead of simply adding the feature maps

from each level that came before it, they are now concatenated and added to the most recent layer. As a result of this, DenseNets are able to reuse features while still necessitating a smaller number of parameters than a standard CNN would require to achieve the same level of performance [25].

C. VGG

The VGG object recognition model is at the bleeding edge of technology and can have as many as 19 layers. VGG, which is a deep CNN, performs better than the baseline on a variety of tasks and datasets, not just ImageNet. The name of the network, VGG, gives away the fact that it is a deep neural network consisting of between 16 and 19 layers [26].

D. ResNet

Deep residual networks (ResNets), like ResNet-50, are 50-layer CNNs. Using shortcut connections, a residual neural network transforms a plain network. Comparatively, ResNets have fewer filters than VGG Nets [25].

E. Inception

Inception is a network with a modular architecture made up of recurrent components called Inception units. It gives the inner layers the freedom to determine which filter size is necessary to acquire the necessary knowledge. So the layer adapts to recognize the object no matter what size it is in the image [27].

F. Xception

By exchanging the traditional Inception components for depthwise Separable Convolutions, Xception augments the inception Style. As with Inception V3, it has large number of parameters [28].

G. NASNet

ResNet integrated residual learning into the conventional CNN framework. The RU, or residual unit, is made up of a standard layer connected via a skip link. By linking the input of one layer directly to its output, the skip connection facilitates the propagation of signals across the network. That's why it is able to train a super-deep model with the help of RUs [29].

H. EfficientNet

All three dimensions of depth, width, and resolution are scaled equally using a compound coefficient in this convolutional neural network design and scaling method. The rationale for the compound scaling approach is the intuitive understanding that a larger input image necessitates a more complex network with more layers to broaden the approachable field and additional channels to pick up the finer details in the larger image [30].

V. Proposed Architecture

Fig. 3 depicts the proposed architecture. Besides the lungs, Chest X-Rays often show other sections of the body, which might complicate the DFE process and reduce the accuracy of the classifier's predictions. U-Net is applied to the issue of X-Ray image segmentation in order to find a solution. The image of the lungs is kept intact during the segmentation process, but the rest of the picture is completely blacked out as shown in Fig. 2.

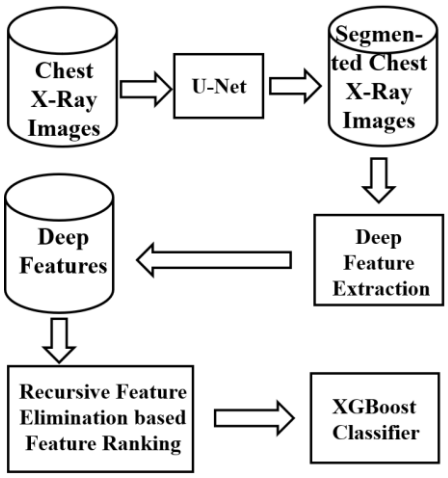

Fig. 3. Proposed Architecture.

Segmented Chest X-Ray images undergo a two-step feature extraction technique. In the first step, a set of segmented X-Ray images is sent to a Pre-Trained model to extract features. As soon as the features have been extracted, they are ranked using Recursive Feature Elimination. At last, it is decided to retain only those features with a ranking of one. This two-step process is described by Algorithm 1 (Deep Feature Extraction).

Algorithm 1: Deep Feature Extraction

Input: Pre-Trained Model (i.e. M), Set of 'N' Images I_1 .. I_N, Required Image Size (i.e., K*K)
Output: Matrix Representing Deep Features after RFE, class_labels
Procedure:

```
M_R ← Remove_Non_Conv_Layers (M)
DF = []
for i=1 to N do
    Resize image I_i to size (K*K)
    features ← M_R (I_i)
    features ← Flatten (features)
    DF ← DF U features
Feature-rank ← Feature-Ranking (DF)
selected-features = DF [feature-rank == 1]
```

In RFE, given an external classifier that assigns weights to features, the primary goal is to determine features by recurrently considering progressively reduced sets of features. The classification model is pre-trained on a limited number of features, and their relative credibility is then established through inspection of a predefined attribute or the execution of a user-defined function. Next, the current set of features is culled to remove the extraneous ones. At last, features are eliminated one by one until only a handful remain.

RFE is a method that relies on a classification model to determine how features should be ranked. Features that aid the classification model in increasing accuracy are ranked higher, whereas features that decrease accuracy are ranked lower. The proposed approach employs the use of REF to guarantee that the output of Pre-Trained models is used to determine the most suitable set of tuning parameters for each variant of the XGBoost classifier model.

The Gradient Boosted decision trees algorithm has been implemented in XGBoost. Here, decision trees are crafted in a logical order. In XGBoost, weights serve a crucial function. All

of the independent variables are given weights, and this information is then used to feed into the decision tree, which makes predictions. Variables that the first decision tree incorrectly predicted are given a higher weight in the second tree's analysis. The ensemble of these separate classifiers/predictors yields a robust and accurate model [31].

Adjustments to the XGBoost Classifier need to be made for a wide range of parameter values so that a precise estimate of inference may be made. In all 29 different parameter values can be tuned for obtaining the best performance of XGBoost model [32]. However, this tuning process requires extremely high processing power in terms of time and computation. Thus, we selected three most widely tuned parameters namely Learning Rate (LR), the number of estimators (classification trees), and the Maximum Depth (MD). The XGBoost Classifier Tuning Algorithm 2 goes into detail about the tuning process. An XGBoost classifier allows the user to modify aspects, including LR, the number of estimators, and MD of each tree.

Algorithm 2: Tune XGBoost Classifier

Input: Matrix Representing Deep Features after RFE, class_labels
Output: XGBoost Classifiers' Finest Tuning Parameters
Procedure:

```
Accuracy-Array = []
for max-depth = 3 to 5 do
    for learning-rate = 0.1 to 0.5 (step-size 0.2) do
        for n-estimator = 300 to 800 (step-size 50) do:
            accuracy-XGB ← XGBoostModelEvalution
            (max_depth, learning_rate, n_estimators)
            Accuracy-Array[n-estimators, learning-rate, max-depth]
            ← accuracy-XGB
Select combinations of Parameters from Accuracy-Array which
gives highest accuracy
```

Having a firm grasp on how our machine learning model operates is becoming increasingly crucial. Merely looking at the model's accuracy as a metric of its efficacy is insufficient, though, because it can mislead you. Black-box models, such as deep CNN, are notoriously challenging to interpret. Local Interpretable Model-agnostic Explanations (LIME) aids in comprehending the operation of classifier model. It denotes the visual features that the model employs to classify the images.

Fig. 4(a) shows features derived from an X-Ray image without lung segmentation, while Figure 4(b) shows features extracted from an X-Ray image with the lungs segmented using U-Net. These images demonstrate how features retrieved from segmented images are superior to those extracted from unsegmented images for training a model.

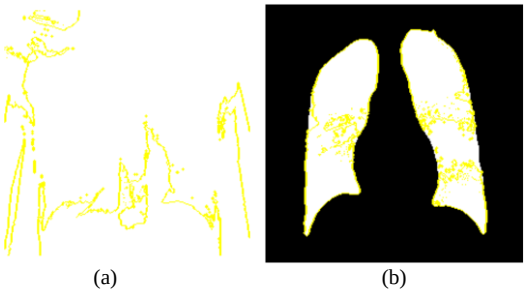

(a) (b)

Fig. 4. (a) Feature Extracted from X-Ray Image without Segmentation by Pre-Trained Model, (b) Feature Extracted from X-Ray Image after Segmentation by Pre-Trained Model.

VI. Experiment Design and Results

In this section, the data utilized for experimentation along with experimental results is discussed. The April 2021 edition of the COVID-19, Pneumonia and Normal Chest X-ray Dataset is drawn upon for this experimentation [33]. In the first step of data collection process, 613 X-ray images of COVID-19 patients were obtained from the following online resources: GitHub [34] [35], Radiopaedia [36], The Cancer Imaging Archive (TCIA) [37], and the Italian Society of Radiology (SIRM) [38]. Then, rather than the data being individually supplemented, a dataset from Mendeley [39] including 912 photos that had previously been augmented was acquired. Finally, 1525 images of pneumonia cases and 1525 X-ray images of normal cases were retrieved from the Kaggle repository [40] and the NIH dataset [41], respectively. The dataset contains 4575 photos, with 1525 images in each of three distinct groups. The dataset's developer gathered these photographs from a wide range of available web resources.

In order to acquire the utmost precise deep feature, which is decisive to ML, the networks MobileNet, MobileNetLarge, MobileNetSmall, DenseNet121, DenseNet169, DenseNet201, Xception, ResNet50V2, ResNet101V2, ResNet152V2, InceptionV3, InceptionResNetV2, VGGNet16, VGGNet19, NASNet, and EfficientNetB0 through EfficientNetB7 were chosen. Effectiveness of model trained for patient classification based on X-Ray images is evaluated using metrics specified in equations 1 to 5.

$$Precision = \frac{TP}{(TP+FP)} \quad (1)$$

$$Recall = \frac{TP}{(TP+FN)} \quad (2)$$

$$Specificity = \frac{TN}{(TN+FP)} \quad (3)$$

$$Accuracy = \frac{(TP+TN)}{(TP+FP+TN+FN)} \quad (4)$$

$$F1 = 2 * \frac{Precision*Recall}{(Precision+Recall)} \quad (5)$$

For validation of proposed approach, experimentation dataset is divided into two parts namely Training Set and Testing Set. Training Set contains randomly selected 70% images (i.e. 3202) where as remaining 30% images (i.e. 1373) are used to test effectiveness of proposed approach. Evaluation metric for every Pre-Trained model are calculated by taking average of 10 iterations of Training-Testing evaluation in which different set of randomly selected images are used for training and testing the proposed approach.

Fig. 5 depicts the precision of tuned XGBoost models that make use of features retrieved by algorithm 1 as well as a variety of pre-trained models. Evidently, the tweaked XGBoost model that was trained using the features that were retrieved by Algorithm 1 and EfficientNetB1 obtains the best precision of 0.964. Results for precision and other evaluation metrics used in this expropriation for EfficientNetB4 to EfficientNetB7 are less compared to any other models. Thus, we have not presented these results in Fig. 5 to Fig. 9.

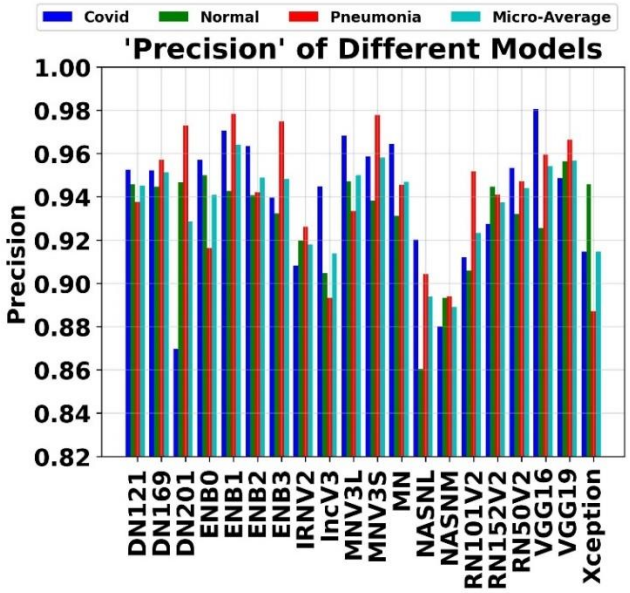

Fig. 5. Precision of Tuned XGBoost Models Trained using Features Extracted by Algorithm 1 (Deep Features Extraction) and Assorted Pre-Trained Models.

Fig. 6 depicts the recall of tuned XGBoost models that make use of features retrieved by algorithm 1 as well as a variety of pre-trained models. Evidently, the tweaked XGBoost model that was trained using the features that were retrieved by Algorithm 1 and EfficientNetB1 obtains the best recall of 0.964.

Fig. 7 depicts the specificity of tuned XGBoost models that make use of features retrieved by algorithm 1 as well as a variety of pre-trained models. Evidently, the tweaked XGBoost model that was trained using the features that were retrieved by Algorithm 1 and EfficientNetB1 obtains the best specificity of 0.982.

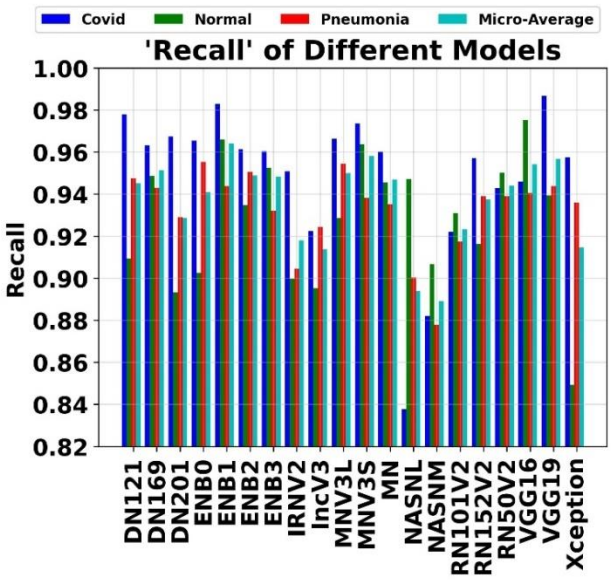

Fig. 6. Recall of Tuned XGBoost Models Trained using Features Extracted by Algorithm 1 (Deep Features Extraction) and Assorted Pre-Trained Models.

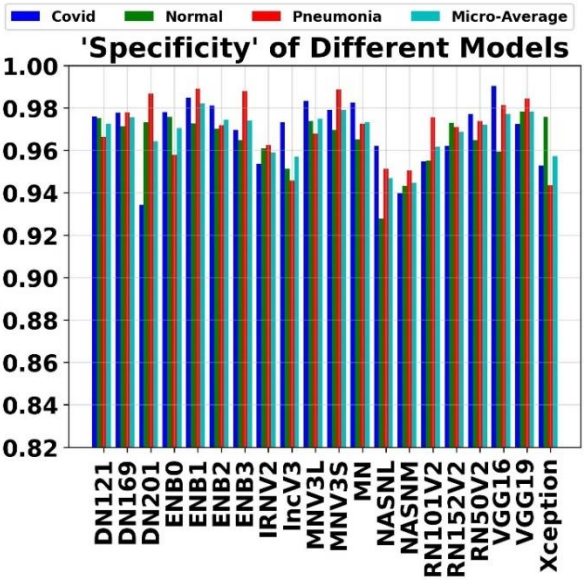

Fig. 7. Specificity of Tuned XGBoost Models Trained using Features Extracted by Algorithm 1 (Deep Features Extraction) and Assorted Pre-Trained Models.

Fig. 8 depicts the accuracy of tuned XGBoost models that make use of features retrieved by algorithm 1 as well as a variety of pre-trained models. Evidently, the tweaked XGBoost model that was trained using the features that were retrieved by Algorithm 1 and EfficientNetB1 obtains the best accuracy of 0.976, which is equivalent to 97.6%.

Fig. 9 depicts the F1-Score of tuned XGBoost models that make use of features retrieved by algorithm 1 as well as a variety of pre-trained models. Evidently, the tweaked XGBoost model that was trained using the features that were retrieved by Algorithm 1 and EfficientNetB1 obtains the best F1-score of 0.964.

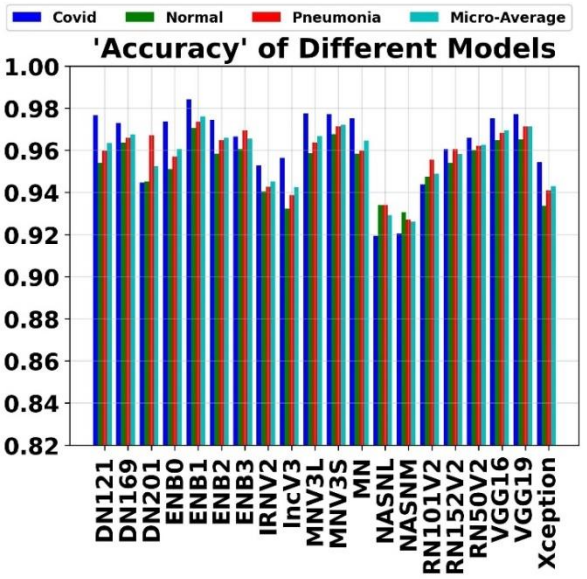

Fig. 8. Accuracy of Tuned XGBoost Models Trained using Features Extracted by Algorithm 1 (Deep Features Extraction) and Assorted Pre-Trained Models.

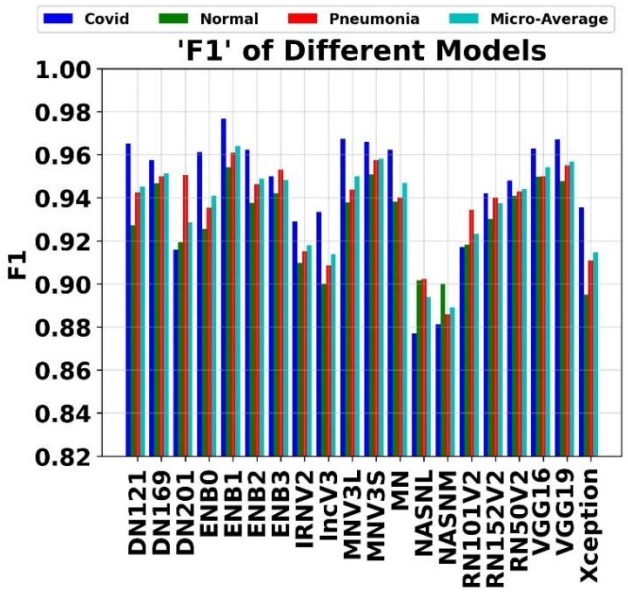

Fig. 9. F1 of Tuned XGBoost Models Trained using Features Extracted by Algorithm 1 (Deep Features Extraction) and Assorted Pre-Trained Models.

Additional set of trained model's (evolution) metrics are provided in table 1 for fine-tuned XGBoost model that was trained using the features that were retrieved by Algorithm 1 and EfficientNetB1. Equations for these metrics are given below in equation 6 to equation 9. These metrics are for provided for individual categories i.e. Covid-19, normal and Pneumonia and well as overall testing dataset.

$$False\ Discovery\ Rate = \frac{FP}{(FP+TP)} \quad (6)$$

$$Negative\ predictive\ value = \frac{TN}{(TN+FN)} \quad (7)$$

$$False\ Negative\ Rate = \frac{FN}{(FN+TP)} \quad (8)$$

$$False\ Positive\ Rate = \frac{FP}{(FP+TN)} \quad (9)$$

TABLE I. EVALUATION METRICS FOR FINE-TUNED XGBOOST MODEL THAT WAS TRAINED USING THE FEATURES THAT WERE RETRIEVED BY ALGORITHM 1 AND EFFICIENTNETB1

Metric	Covid-19	Normal	Pneumonia	Micro-Average
Accuracy	98.4%	97.1%	97.3%	97.6%
F1	0.977	0.954	0.961	0.964
Precision	0.971	0.943	0.979	0.964
Recall	0.983	0.966	0.944	0.964
Specificity	0.985	0.973	0.989	0.982
False Discovery Rate	0.029	0.057	0.021	0.036
Negative Predictive Value	0.991	0.984	0.971	0.982
False Negative Rate	0.017	0.034	0.056	0.036
False Positive Rate	0.015	0.027	0.011	0.018

TABLE II. COMPARISON OF PROPOSED METHODOLOGY WITH RELATED WORK

Reference	Method	Dataset	Accuracy
[1]	22-Layer CNN	Merged Publicly Available Datasets	94.2%
[9]	VGG16 + CLAHE	Merged Publicly Available Datasets	88.8%
[10]	Xception + ResNet50V2	Merged Publicly Available Datasets	91.4%
[11]	DenseNet-121	Merged Publicly Available Datasets	81.04%
[12]	ResNet50V2 + VGG-16 + InceptionV3	Merged Publicly Available Datasets	95.49%
[13]	VGG16	Publicly available Dataset	91.69%
[14]	COVID-GATNet	Merged Publicly Available Datasets	94.1%
[15]	VGG16	Publicly available Dataset	91.0%
[16]	DenseNet169	Publicly available Dataset	95.72
[17]	AlexNet	Merged Publicly Available Datasets	94.0%
[18]	Xception	Merged Publicly Available Datasets	89.6%
[20]	EfficientNetB3	Merged Publicly Available Datasets	93.9%
Proposed	U-NET + EfficientNetB1 + XGBoost	Merged Publicly Available Datasets	97.6%

Table II details how the proposed architecture and experimental results compare to the state-of-the-art. Because there is no universally accepted reference dataset, it is clear that all researchers are making use of data that is already available publicly.

VII. DISCUSSION

Significant research contributions of this paper are as follows:

1) Proposed use of U-Net model to segment lung part from X-Ray image and then segmented image to extract deep features.

2) Proposed model is trained on reduced features set using XGBoost classifier model, thus it can be easily deployed on low-end cost-efficient devices like Raspberry-pi easily.

3) Use of Explainable AI: Local Interpretable Model-agnostic Explanations (LIME) methodology is used to explain the decision-making process of Deep Learning Model (Explained in section V).

4) Performance of 20 different Pre-Trained models is evaluated against 9 different metrics specified in Table I.

Limitations of the Research work carried out are as follows:

1) As discussed in Section V, the XGBoost model has 29 parameters that can be adjusted to optimize performance. This study, however, relied on only three variables. This allows for

additional investigation into how the remaining XGBoost classifier parameters affect performance.

2) Using the U-Net model for segmentation does not result in any image enhancement of the lung segment area. Pre-Trained models for deep feature extraction can be used after various image enhancement techniques on lung segmented images have been performed.

VIII. Conclusion

In this study, a Deep Feature Extraction-based method for detecting individuals infected with Covid-19 and pneumonia by analyzing Chest X-Rays is provided. U-Net is used to split the lung region of the chest from the image so that the Pre-Trained model may concentrate on the relevant area of the image and extract more meaningful features. In this article, following the segmentation of the lung part, a two-stage technique to the extraction of deep features from X-Ray images is provided. After that, the XGBoost classifiers are trained to exploit these features in order to differentiate between patients infected with Covid-19 and healthy individuals and patients infected with pneumonia. When the performance of 20 different Pre-Trained models is analyzed, it is discovered that the maximum detection accuracy, precision, recall, specificity, and F1-score are achieved when EfficientNetB1 is used to extract deep features. The respective values for these metrics are 97.6%, 0.964, 0.964, and 0.982. These findings lend credence to the efficiency of the strategy that was proposed.

References

[1] E. Hussain, M. Hasan, M. A. Rahman, I. Lee, T. Tamanna, and M. Z. Parvez, "CoroDet: A deep learning based classification for COVID-19 detection using chest X-ray images," Chaos, Solitons and Fractals, vol. 142, 2021, doi: 10.1016/j.chaos.2020.110495.

[2] "https://www.worldometers.info/coronavirus/worldwide-graphs/.".

[3] A. M. Ismael and A. Şengür, "Deep learning approaches for COVID-19 detection based on chest X-ray images," Expert Syst. Appl., vol. 164, 2021, doi: 10.1016/j.eswa.2020.114054.

[4] A. Maier, C. Syben, T. Lasser, and C. Riess, "A gentle introduction to deep learning in medical image processing," Zeitschrift fur Medizinische Physik, vol. 29, no. 2. pp. 86–101, 2019, doi: 10.1016/j.zemedi.2018.12.003.

[5] K. Weiss, T. M. Khoshgoftaar, and D. D. Wang, "A survey of transfer learning," J. Big Data, vol. 3, no. 1, 2016, doi: 10.1186/s40537-016-0043-6.

[6] E. Deniz, A. Şengür, Z. Kadiroğlu, Y. Guo, V. Bajaj, and Ü. Budak, "Transfer learning based histopathologic image classification for breast cancer detection," Heal. Inf. Sci. Syst., vol. 6, no. 1, 2018, doi: 10.1007/s13755-018-0057-x.

[7] Z. Li, F. Liu, W. Yang, S. Peng, and J. Zhou, "A Survey of Convolutional Neural Networks: Analysis, Applications, and Prospects," IEEE Trans. Neural Networks Learn. Syst., pp. 1–21, 2021, doi: 10.1109/tnnls.2021.3084827.

[8] C. Ieracitano et al., "A fuzzy-enhanced deep learning approach for early detection of Covid-19 pneumonia from portable chest X-ray images," Neurocomputing, vol. 481, pp. 202–215, Apr. 2022, doi: 10.1016/j.neucom.2022.01.055.

[9] F. Saiz and I. Barandiaran, "COVID-19 Detection in Chest X-ray Images using a Deep Learning Approach," Int. J. Interact. Multimed. Artif. Intell., vol. 6, no. 2, p. 4, 2020, doi: 10.9781/ijimai.2020.04.003.

[10] M. Rahimzadeh and A. Attar, "A modified deep convolutional neural network for detecting COVID-19 and pneumonia from chest X-ray images based on the concatenation of Xception and ResNet50V2," Informatics Med. Unlocked, vol. 19, 2020, doi: 10.1016/j.imu.2020.100360.

[11] A. Haghanifar, M. M. Majdabadi, Y. Choi, S. Deivalakshmi, and S. Ko, "COVID-CXNet: Detecting COVID-19 in frontal chest X-ray images using deep learning," Multimed. Tools Appl., vol. 81, no. 21, pp. 30615–30645, Sep. 2022, doi: 10.1007/s11042-022-12156-z.

[12] M. Shorfuzzaman, M. Masud, H. Alhumyani, D. Anand, and A. Singh, "Artificial Neural Network-Based Deep Learning Model for COVID-19 Patient Detection Using X-Ray Chest Images," J. Healthc. Eng., vol. 2021, 2021, doi: 10.1155/2021/5513679.

[13] M. D. K. Hasan et al., "Deep Learning Approaches for Detecting Pneumonia in COVID-19 Patients by Analyzing Chest X-Ray Images," Math. Probl. Eng., vol. 2021, 2021, doi: 10.1155/2021/9929274.

[14] J. Li, D. Zhang, Q. Liu, R. Bu, and Q. Wei, "COVID-GATNet: A Deep Learning Framework for Screening of COVID-19 from Chest X-Ray Images," in 2020 IEEE 6th International Conference on Computer and Communications, ICCC 2020, 2020, pp. 1897–1902, doi: 10.1109/ICCC51575.2020.9345005.

[15] D. Dansana et al., "Early diagnosis of COVID-19-affected patients based on X-ray and computed tomography images using deep learning algorithm," Soft Comput., 2020, doi: 10.1007/s00500-020-05275-y.

[16] K. Hammoudi et al., "Deep Learning on Chest X-ray Images to Detect and Evaluate Pneumonia Cases at the Era of COVID-19," J. Med. Syst., vol. 45, no. 7, 2021, doi: 10.1007/s10916-021-01745-4.

[17] A. U. Ibrahim, M. Ozsoz, S. Serte, F. Al-Turjman, and P. S. Yakoi, "Pneumonia Classification Using Deep Learning from Chest X-ray Images During COVID-19," Cognit. Comput., 2021, doi: 10.1007/s12559-020-09787-5.

[18] A. I. Khan, J. L. Shah, and M. M. Bhat, "CoroNet: A deep neural network for detection and diagnosis of COVID-19 from chest x-ray images," Comput. Methods Programs Biomed., vol. 196, 2020, doi: 10.1016/j.cmpb.2020.105581.

[19] H. Panwar, P. K. Gupta, M. K. Siddiqui, R. Morales-Menendez, P. Bhardwaj, and V. Singh, "A deep learning and grad-CAM based color visualization approach for fast detection of COVID-19 cases using chest X-ray and CT-Scan images," Chaos, Solitons and Fractals, vol. 140, 2020, doi: 10.1016/j.chaos.2020.110190.

[20] E. Luz et al., "Towards an effective and efficient deep learning model for COVID-19 patterns detection in X-ray images," Res. Biomed. Eng., vol. 38, no. 1, pp. 149–162, Mar. 2022, doi: 10.1007/s42600-021-00151-6.

[21] S. Rajaraman and S. Antani, "Weakly labeled data augmentation for deep learning: A study on COVID-19 detection in chest X-rays," Diagnostics, vol. 10, no. 6, 2020, doi: 10.3390/diagnostics10060358.

[22] S. H. Kassania, P. H. Kassanib, M. J. Wesolowskic, K. A. Schneidera, and R. Detersa, "Automatic Detection of Coronavirus Disease (COVID-19) in X-ray and CT Images: A Machine Learning Based Approach," Biocybern. Biomed. Eng., vol. 41, no. 3, pp. 867–879, 2021, doi: 10.1016/j.bbe.2021.05.013.

[23] O. Ronneberger, P. Fischer, and T. Brox, "U-net: Convolutional networks for biomedical image segmentation," in Lecture Notes in Computer Science (including subseries Lecture Notes in Artificial Intelligence and Lecture Notes in Bioinformatics), 2015, vol. 9351, pp. 234–241, doi: 10.1007/978-3-319-24574-4_28.

[24] D. Sinha and M. El-Sharkawy, "Thin MobileNet: An Enhanced MobileNet Architecture," in 2019 IEEE 10th Annual Ubiquitous Computing, Electronics and Mobile Communication Conference, UEMCON 2019, 2019, pp. 0280–0285, doi: 10.1109/UEMCON47517.2019.8993089.

[25] C. Zhang et al., "ResNet or DenseNet? Introducing dense shortcuts to ResNet," in Proceedings - 2021 IEEE Winter Conference on Applications of Computer Vision, WACV 2021, 2021, pp. 3549–3558, doi: 10.1109/WACV48630.2021.00359.

[26] S. Pasban, S. Mohamadzadeh, J. Zeraatkar-Moghaddam, and A. K. Shafiei, "Infant brain segmentation based on a combination of vgg-16 and u-net deep networks," IET Image Process., vol. 14, no. 17, pp. 4756–4765, 2020, doi: 10.1049/iet-ipr.2020.0469.

[27] Z. Ying et al., "Tai-sarnet: Deep transferred atrous-inception cnn for small samples sar atr," Sensors (Switzerland), vol. 20, no. 6, 2020, doi: 10.3390/s20061724.

[28] F. Chollet, "Xception: Deep learning with depthwise separable convolutions," in Proceedings - 30th IEEE Conference on Computer Vision and Pattern Recognition, CVPR 2017, 2017, vol. 2017–Janua, pp. 1800–1807, doi: 10.1109/CVPR.2017.195.

[29] F. Martínez, F. Martínez, and E. Jacinto, "Performance evaluation of the NASnet convolutional network in the automatic identification of COVID-19," Int. J. Adv. Sci. Eng. Inf. Technol., vol. 10, no. 2, pp. 662–667, 2020, doi: 10.18517/ijaseit.10.2.11446.

[30] M. Tan and Q. V. Le, "EfficientNet: Rethinking model scaling for convolutional neural networks," in 36th International Conference on Machine Learning, ICML 2019, 2019, vol. 2019–June, pp. 10691–10700.

[31] T. Chen and C. Guestrin, "XGBoost: A scalable tree boosting system," in Proceedings of the ACM SIGKDD International Conference on Knowledge Discovery and Data Mining, 2016, vol. 13–17–Augu, pp. 785–794, doi: 10.1145/2939672.2939785.

[32] "No Title." https://xgboost.readthedocs.io/en/stable/parameter.html.

[33] Z. Asraf, Amanullah; Islam, "COVID19, Pneumonia and Normal Chest X-ray PA Dataset," Mendeley Data, V1, 2021, doi: 10.17632/jctsfj2sfn.1.

[34] http://arxiv.org/abs/2003.11597.

[35] https://github.com/agchung.

[36] https://radiopaedia.org/.

[37] https://www.cancerimagingarchive.net/.

[38] https://www.sirm.org/en/category/articles/covid-19-database/.

[39] https://data.mendeley.com/datasets/2fxz4px6d8/4.

[40] https://www.kaggle.com/paultimothymooney/chest-xray-pneumonia.

[41] https://www.kaggle.com/nih-chest-xrays/data.